Classical and quantum-mechanical treatments of the energy loss of charged particles in dilute plasmas

Leonardo de Ferrariis and Néstor R. Arista
Centro Atómico Bariloche and Instituto Balseiro,
Comisión Nacional de Energía Atómica y Universidad Nacional de Cuyo,
8400 Bariloche, Rio Negro, Argentina
(Received 26 May 1983)

We calculate the energy loss of charged particles in nondegenerate plasmas using classical and quantum-mechanical approximations. First we consider classical binary collisions between the test particle and the particles in the plasma, and obtain the energy transferred as a function of the relative velocity. This is integrated over the thermal distribution of plasma-particle velocities using simple analytical approximations. Then we use the quantum-mechanical analysis of the scattering of partial waves to find the transport cross section for a screened potential, and introduce analytical approximations to calculate the phase shifts. The thermal average is also calculated analytically. The study yields simple expressions for the energy loss in terms of the velocity and charge of the particle and of the density and temperature of the plasma. In particular, we retrieve various results of previous authors, which apply as limiting cases in the classical or quantum-mechanical regimes. The transition between these cases is described by analytical expressions of excellent accuracy. The calculation is finally compared with experimental results from laboratory plasmas in the classical domain.

I. INTRODUCTION

The problem of energy loss of fast particles in plasmas has been studied by many authors using a variety of approximations, and applications have been considered over wide ranges of plasma densities and temperatures, which include the various conditions of interest for astrophysics (stellar and interstellar media), solid-state plasmas, cold and hot laboratory plasmas, and, in particular, the extreme conditions of interest for current studies of inertial and magnetic confinement of plasmas.[1,2] In terms of classical mechanics, the rate of energy relaxation of a charged particle in a plasma was given by Spitzer,[3] based on earlier results of Chandrasekhar,[4] who studied the analogous problem of the energy relaxation of a star moving in the presence of the gravitational perturbations from a cluster of stars. Further descriptions along similar lines were given by Gryzinski[5] and Butler and Buckingham[6] by considering binary collisions of the charged particle with the electrons and ions in the plasma.

On the other hand, a dielectric formulation of the energy-loss rate was studied by Pines and Bohm,[7] Akhiezer and Sitenko,[8] and other workers for the case of dilute plasmas, and by Lindhard[9] and Ritchie[10] for degenerate plasmas. More recently, Skupsky,[11] Arista and Brandt,[2] and Maynard and Deutsch[12] have considered the calculation of the energy loss and straggling in a quantum-mechanical plasma of arbitrary degeneracy. These calculations contain a description of short-range interactions in terms of quantum plane waves for the scattered electrons.

Other descriptions of the energy-loss rate in dilute plasmas, incorporating both short-range collisions and collective phenomena, were given in a series of papers by Kihara, Aono, Itikawa, and Honda[13–16] and by May.[17] They were based on Hubbard's observation[18] that there is a broad overlapping region between the dielectric and the binary-collision treatments of the problem, leading to a unified description of the energy loss in terms of a velocity-dependent Coulomb logarithm ($\ln\Lambda$). Further developments were made by Hamada *et al.*,[19–21] who gave the energy loss to plasma electrons in terms of tabulated functions, for the whole range of nonrelativistic velocities and incorporating quantum diffraction effects on close collisions. This contributes to filling the gap between previous classical and quantum-mechanical approximations to the Coulomb logarithm.

It is the purpose of this paper to provide complete analytical results that apply to all these conditions of interest and, hence, permit rapid evaluations of energy-loss rates, ranges, stopping times, and related quantities over wide ranges of ion velocities and plasma densities and temperatures.

To illustrate the different conditions of interest and the corresponding physical parameters, let us consider a test ion of charge Z_1e and velocity v, in an electron plasma of density n and temperature T, and let $v_e=(2k_BT/m)^{1/2}$ represent the thermal velocities of the electrons (v_e gives the most probable velocity for the Maxwell-Boltzmann distribution). If the velocity of the ion exceeds the thermal velocity v_e, the energy loss per unit distance (plasma stopping power) is given by

$$-\frac{dE}{dx}=\frac{4\pi nZ_1^2e^4}{mv^2}\ln\Lambda(v),\quad v\gg v_e \tag{1}$$

and in the opposite case

$$-\frac{dE}{dx}=\tfrac{16}{3}\pi^{1/2}\frac{nZ_1^2e^4m^{1/2}v}{(2k_BT)^{3/2}}\ln\Lambda(0),\quad v\ll v_e \tag{2}$$

where k_B is the Boltzmann constant. Simple expressions for the velocity-dependent collision logarithm $\ln\Lambda$ can be given in each case by using either classical or quantum-mechanical (plane-wave) approximations. In particular, in an impact-parameter description the result becomes of the form

$$\ln\Lambda=\ln(b_2/b_1)\,, \tag{3}$$

where the values of the maximum and minimum impact parameters for each case are as follows.

(a) $v\gg v_e$, classical approximation:

$$b_1\cong b_c=\frac{Z_1e^2}{mv^2},\quad b_2\cong\lambda_{ad}=\frac{v}{\omega_p}\,. \tag{4a}$$

(b) $v\ll v_e$, classical approximation:

$$b_1\cong b_c=\frac{Z_1e^2}{mv_e^2}=\frac{Z_1e^2}{2k_BT},\quad b_2\cong\lambda_D=\left[\frac{k_BT}{4\pi ne^2}\right]^{1/2}\simeq\frac{v_e}{\omega_p}\,. \tag{4b}$$

(c) $v\gg v_e$, quantum-mechanical approximation:

$$b_1\cong\lambda=\frac{\hbar}{mv},\quad b_2\cong\lambda_{\rm ad}=\frac{v}{\omega_p}\,. \tag{4c}$$

(d) $v\ll v_e$, quantum-mechanical approximation:

$$b_1\cong\lambda_e=\frac{\hbar}{mv_e},\quad b_2\cong\lambda_D=\left[\frac{k_BT}{4\pi ne^2}\right]^{1/2}\simeq\frac{v_e}{\omega_p}\,. \tag{4d}$$

Here $\lambda_D=(k_BT/4\pi ne^2)^{1/2}$ is the Debye screening length and

$$\omega_p=(4\pi ne^2/m)^{1/2}$$

is the plasma frequency; namely, the frequency of long-wavelength collective electron oscillations.

From Eqs. (4) we notice that the distinction between classical and quantum-mechanical results arises solely through the minimum impact parameter b_1, since it is only in the short-range domain where one should consider possible quantum diffraction effects on the electron trajectories. This is, in fact, the origin of the well-known discrepancy between the Bohr[22] and Bethe[23] formulas for the energy loss of fast charged particles. As in the solution given by Bloch,[24,25] the important parameter here becomes

$$\eta=\frac{b_{\rm CL}}{b_{\rm QM}}=\frac{b_c}{\lambda}=\frac{Z_1e^2}{\hbar v_r}\,, \tag{5}$$

where v_r denotes a mean relative velocity between the ion and the electrons (in particular $v_r=v$ if $v\gg v_e$, and $v_r=v_e$ if $v\ll v_e$), CL represents the classical approximation, and QM represents the quantum-mechanical approximation. The value $\eta=1$ separates the domains of applicability of the previously mentioned classical ($\eta\gg1$) and quantum-mechanical ($\eta\ll1$) approximations.

For large velocities, $v\gg v_e$, $\eta\cong Z_1e^2/\hbar v$ depends only on the parameters of the ion; in this case the quantum-mechanical result applies for $v>Z_1e^2/\hbar=Z_1v_0$ ($v_0=e^2/\hbar=$Bohr velocity). On the other hand, for slow ions, $v\ll v_e$,

$$\eta\cong\frac{Z_1e^2}{\hbar v_e}=\frac{Z_1e^2}{\hbar}\left[\frac{m}{2k_BT}\right]^{1/2}, \tag{6}$$

and hence the quantum-mechanical result applies at high plasma temperatures,

$$2k_BT\gg Z_1^2me^4/\hbar^2=Z_1^2E_0\,,$$

where $E_0=me^4/\hbar^2=1$ a.u.$=27.2$ eV. For protons this corresponds to electron temperatures larger than 10^5 K (cf. Fig. 1 of Ref. 2). Moreover, as the charge of the ion increases, the transition between the classical and quantum-mechanical regimes appears at increasingly higher plasma temperatures, reaching the regions of interest for fusion reactors when $Z_1\gtrsim10$.

Another point of interest in Eqs. (4a)–(4d) is the transition between static and dynamical screening effects. This becomes apparent through the value of b_2. At low velocities, $v<v_e$, the Coulomb field of the ion is adiabatically screened by the electrons over a distance given by the Debye length

$$\lambda_D=(k_BT/4\pi ne^2)^{1/2}\,.$$

With increasing ion velocities the screening becomes less effective and, for $v>v_e$, it gives rise to a wake of dynamical polarization in the plasma[7]; in these conditions the field of the ion becomes effective over increasing distances as given by the adiabatic length[26,27] $\lambda_{\rm ad}=v/\omega_p$. In fact, for distances $\rho>\lambda_{\rm ad}$ away from the ion trajectory, the perturbation acts over a time $\Delta t\sim\rho/v$ that exceeds the response time of the plasma $\sim\omega_p^{-1}$, leading again to an adiabatic response of the medium that shields the external field. The transition between these two cases can be studied in detail only through numerical examples due to the many-body character of the problem.

In summary, the expressions for $\ln\Lambda$ in Eqs. (1) and (2), with the values given in Eqs. (4a)–(4d), can be written as follows.

(i) Classical results ($\eta=Z_1e^2/\hbar v_r\gg1$):

$$\ln\Lambda=\begin{cases}\ln\left[\dfrac{1.123mv^3}{Z_1e^2\omega_p}\right], & v\gg v_e \qquad (7a)\\[2ex] \ln\left[\dfrac{4(k_BT)^{3/2}}{Z_1e^2\omega_pm^{1/2}}\right]-2\gamma-\frac{1}{2}, & v\ll v_e\,. \qquad (7b)\end{cases}$$

(ii) Quantum-mechanical results ($\eta=Z_1e^2/\hbar v_r\ll1$):

$$\ln\Lambda=\begin{cases}\ln\left[\dfrac{2mv^2}{\hbar\omega_p}\right], & v\gg v_e \qquad (8a)\\[2ex] \ln\left[\dfrac{k_BT}{\hbar\omega_p}\right]+\dfrac{1}{4}, & v\ll v_e\,. \qquad (8b)\end{cases}$$

Correction terms of numerical interest have been included so as to cast these results in the more exact forms given in Refs. 8, 13, 9, and 2, respectively.

In this paper we develop approximations that comprise these various results. In Sec. II the energy loss of an ion moving in a plasma is described in terms of a relative-velocity-dependent transport cross section. The problem is then studied using classical mechanics, Sec. III, and using the quantum phase-shifts method, Sec. IV. In both cases we introduce approximations that lead to final analytical expressions for the energy loss per unit distance. These results are analyzed in Sec. V, where we also retrieve the particular cases studied by previous authors and we compare with experimental results. Finally, in Sec. VI we summarize our results and conclusions.

II. TRANSPORT CROSS SECTION AND ENERGY LOSS

In this section we obtain a general expression for the energy-loss rate of a charged particle in a plasma as an integral over a thermal distribution of plasma particles (electrons or ions) and in terms of a relative-velocity dependent transport cross section. Let us consider the collision between a test particle of charge Z_1e, mass m_1, and velocity $\vec{v}_1$, with a plasma particle of charge Z_2e, mass m_2, and velocity $\vec{v}_2$, as shown in Fig. 1. The kinetic energy "gained" by particle 1 in the collision is

$$\Delta E=\frac{1}{2m_1}(p_1'^2-p_1^2)=\frac{1}{2m_1}(\vec{p}_1+\vec{p}\,'_1)\cdot\Delta\vec{p}_1 , \tag{9}$$

where primes are used to denote the values after the collision, $\Delta\vec{p}_1=\vec{p}\,'_1-\vec{p}_1$ is the change in the momentum of particle 1. By introducing the relative velocity $\vec{v}_r$ and the center-of-mass (c.m.) velocity $\vec{v}_{\text{c.m.}}$,

$$\vec{v}_r=\vec{v}_2-\vec{v}_1=v_r\hat{n} , \tag{10}$$

$$\vec{v}_{\text{c.m.}}=(m_1\vec{v}_1+m_2\vec{v}_2)/(m_1+m_2) , \tag{11}$$

we obtain

$$\begin{aligned}\vec{p}_1&=m_1\vec{v}_{\text{c.m.}}-\mu v_r\hat{n} ,\\ \vec{p}\,'_1&=m_1\vec{v}_{\text{c.m.}}-\mu v_r\hat{n}' ,\end{aligned} \tag{12}$$

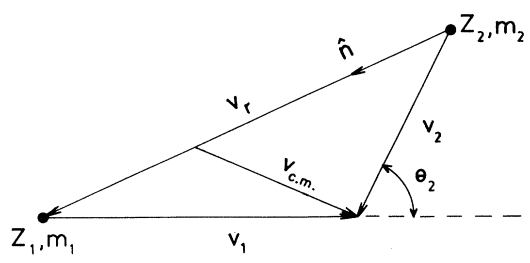

FIG. 1. Illustration of the variables in the text. Incident particle with charge Z_1e, mass m_1, and velocity v_1. Plasma particle with charge Z_2e, mass m_2, and velocity v_2, moving with angle θ_2. The relative velocity v_r and the center-of-mass velocity $v_{\text{c.m.}}$ are also indicated.

where $\hat{n}$ is a unit vector in the direction of $\vec{v}_r$ (see Fig. 1) and $\mu=m_1m_2/(m_1+m_2)$ is the reduced mass.

Using these values in Eq. (9) we get

$$\Delta E=\mu v_r(\hat{n}-\hat{n}')\cdot\vec{v}_{\text{c.m.}}=\Delta\vec{p}_1\cdot\vec{v}_{\text{c.m.}} . \tag{13}$$

Let us now calculate $\Delta\vec{p}_1$ in the c.m. frame. It is convenient here to consider many plasma particles incident with the same velocity $\vec{v}_r$ but with different impact parameters. By symmetry the sum of $\Delta\vec{p}_1$ for all these particles will be in the direction of $\hat{n}$; we then simplify the problem by calculating only this component, namely,

$$\Delta p_{1n}=\Delta\vec{p}_1\cdot\hat{n}=\mu v_r(1-\hat{n}\cdot\hat{n}')=\mu v_r(1-\cos\theta) , \tag{14}$$

where θ is the angle of scattering in the c.m. system.

We can now relate Δp_{1n} to the transport cross section $\sigma_{\text{tr}}(v_r)$, or momentum-transfer cross section, by integrating over impact parameters,

$$\Delta p_{1n}=\mu v_r\int(1-\cos\theta)2\pi b\,db=\mu v_r\sigma_{tr}(v_r) , \tag{15}$$

where $\sigma_{\text{tr}}(v_r)=\int(1-\cos\theta)d\sigma$.

Taking into account the flux of plasma particles incident with angle θ_2 and within a time interval Δt, we obtain the momentum transfer corresponding to those particles:

$$\Delta\vec{p}_{\theta_2}=\Delta p_{1n}dN_2v_r\Delta t\hat{n} . \tag{16}$$

By Eq. (13) we obtain the energy transfer in the laboratory system corresponding also to those particles:

$$\Delta E_{\theta_2}=\Delta\vec{p}_{\theta_2}\cdot\vec{v}_{\text{c.m.}}=(\hat{n}\cdot\vec{v}_{\text{c.m.}})\Delta p_{1n}dN_2v_r\Delta t , \tag{17}$$

where dN_2 denotes the fraction of particles incident with angles around θ_2,φ_2. For an isotropic distribution of plasma particles in the laboratory system, and integrating over the angle φ_2, we can set

$$dN_2=\frac{1}{4\pi}\sin\theta_2d\theta_2d\varphi_2=\tfrac{1}{2}\sin\theta_2d\theta_2 . \tag{18}$$

Using Eqs. (10) and (11) we obtain

$$(\hat{n}\cdot\vec{v}_{\text{c.m.}})=\frac{v_r}{2}\left[\frac{v_2^2-v_1^2}{v_r^2}-\frac{m_1-m_2}{m_1+m_2}\right] , \tag{19}$$

and integrating Eq. (17) over the angle of incidence θ_2 we get the energy-loss rate as follows:

$$-\frac{\Delta E}{\Delta t}=\tfrac{1}{4}\int_0^\pi d\theta_2\sin\theta_2\left[\frac{m_1-m_2}{m_1+m_2}+\frac{v_1^2-v_2^2}{v_r^2}\right]\times\mu v_r^3\sigma_{\text{tr}}(v_r) . \tag{20}$$

It is convenient to transform this into an integral over relative velocities v_r,

$$|v_1-v_2|<v_r<v_1+v_2 .$$

From Fig. 1, we can write

$$v_r^2=v_1^2+v_2^2+2v_1v_2\cos\theta_2$$

and then

$$\sin\theta_2 d\theta_2 = -v_r dv_r / v_1 v_2 ,$$

which yields

$$-\frac{dE}{dt} = \frac{\mu}{4v_1 v_2} \int_{|v_1 - v_2|}^{v_1+v_2} dv_r v_r^4 \sigma_{\rm tr}(v_r) \times \left[\frac{m_1 - m_2}{m_1 + m_2} + \frac{v_1^2 - v_2^2}{v_r^2} \right] . \quad (21)$$

To write this in a more familiar way we can now advance a result from the next two sections, namely,

$$\sigma_{\rm tr}(v_r) = 4\pi b_c^2 \ln\Lambda_{\rm tr}(v_r) = 4\pi \left[\frac{Z_1 Z_2 e^2}{\mu v_r^2} \right]^2 \ln\Lambda_{\rm tr}(v_r) , \quad (22)$$

and from Eq. (21) we obtain

$$-\frac{dE}{dx} = -\frac{1}{v_1}\frac{dE}{dt} = 4\pi \frac{(Z_1 Z_2 e^2)^2}{\mu v_1^2} G(v_1, v_2) \quad (23)$$

with

$$G(v_1, v_2) = \frac{1}{4v_2} \int dv_r \left[\frac{m_1 - m_2}{m_1 + m_2} + \frac{v_1^2 - v_2^2}{v_r^2} \right] \ln\Lambda_{\rm tr}(v_r) . \quad (24)$$

Finally, we calculate the mean energy loss per unit distance S—i.e., the stopping power—as the average over the thermal distribution of plasma-particle velocities, viz.,

$$S \equiv -\left\langle \frac{dE}{dx} \right\rangle = 4\pi \frac{(Z_1 Z_2 e^2)^2}{\mu v_1^2} n_2 G(v_1) , \quad (25)$$

where

$$G(v_1) = \langle G(v_1, v_2) \rangle = \int_0^\infty dv_2 N(v_2) G(v_1, v_2) , \quad (26)$$

and

$$N(v_2) dv_2 = \left[\frac{m_2}{2\pi k_B T} \right]^{3/2} \exp\left[\frac{-m v_2^2}{2 k_B T} \right] 4\pi v_2^2 dv_2 \quad (27)$$

in terms of the temperature T and of the density n_2 of the particles in the plasma.

III. CLASSICAL THEORY

We now consider the classical problem of scattering of a plasma particle of charge $Z_2 e$, reduced mass μ, and velocity v_r on a center of charge $Z_1 e$. For close collisions, the angle of deflection θ in the c.m. system is related to the impact parameter b by the Rutherford relation

$$\cos\theta = (b - b_c)^2 / (b^2 + b_c^2) , \quad (28)$$

where

$$b_c = Z_1 Z_2 e^2 / \mu v_r^2 . \quad (29)$$

This yields a transport cross section, by Eq. (15),

$$\sigma_{\rm tr}^{\rm CL}(v_r) = 4\pi b_c^2 \int_0^\infty \frac{b}{b^2 + b_c^2} db . \quad (30)$$

The logarithmic divergence of this integral, for $b \to \infty$, can be avoided with the use of a more realistic potential in the plasma, taking into account the effect of the screening in reducing the range of the fields to a finite distance λ_s. In general, for a moving ion, this can only be done in an approximate way. With these limitations in mind we restrict the integration of Eq. (30) to impact parameters smaller than $b_{\max} \sim \lambda_s$, whose value—to be discussed later—depends on the ion velocity v_1, but not on the relative velocity v_r; this is a consequence of the collective response of the plasma. Thus, Eq. (30) yields

$$\sigma_{\rm tr}^{\rm CL}(v_r) = 2\pi b_c^2 \ln(1 + \alpha^2 v_r^4) \quad (31)$$

with

$$\alpha = \mu b_{\max} / Z_1 Z_2 e^2 . \quad (32)$$

Using the value $\frac{1}{2}\ln(1+\alpha^2 v_r^4)$ for the collision logarithm in Eqs. (22) and (24) we obtain

$$G(v_1, v_2) = \frac{1}{8v_2} \int_{|v_1 - v_2|}^{v_1+v_2} dv_r \left[\frac{m_1 - m_2}{m_1 + m_2} + \frac{v_1^2 - v_2^2}{v_r^2} \right] \times \ln(1 + \alpha^2 v_r^4) . \quad (33)$$

This integral can be calculated analytically, as it was first done by Gryzinsky,[5] with the following result:

$$G[r,s] = \frac{1}{4d} \left\{ \frac{M - rs}{\sqrt{2}} \left[\arctan\left[\frac{\sqrt{2}s}{1 - s^2} \right] - \arctan\left[\frac{\sqrt{2}|r|}{1 - r^2} \right] \right] + \frac{M + rs}{\sqrt{2}} \left[\ln\left[\frac{s^2 + \sqrt{2}s + 1}{(1 + s^4)^{1/2}} \right] - \ln\left[\frac{r^2 + \sqrt{2}|r| + 1}{(1 + r^4)^{1/2}} \right] \right] + \frac{1}{2}(r + Ms)\ln(1 + s^4) - \frac{1}{2}\left[\frac{rs}{|r|} + M|r| \right] \ln(1 + r^4) - 2M(s - |r|) \right\} , \quad (34)$$

where

$$M=\frac{m_1-m_2}{m_1+m_2}\ ,\quad r=d(1-w),\quad s=d(1+w)\ ,$$
$$d=\alpha^{1/2}v_2,\quad w=v_1/v_2\ . \tag{35}$$

Two useful approximations for the cases $v_1 \gg v_2$ and $v_1 \ll v_2$ can now be obtained by expanding the integral of Eq. (33), which yields

$$G(v_1 \gg v_2)\cong\left[\frac{1}{2}-\frac{\delta}{4}\right]\ln(1+\alpha^2 v_1^4)\ , \tag{36a}$$

$$G(v_1 \ll v_2)\cong-\frac{\delta}{4}\left[\frac{v_1}{v_2}\right]\ln(1+\alpha^2 v_2^4)+\frac{2}{3}\left[\frac{v_1}{v_2}\right]^3 \tag{36b}$$

with

$$\delta=2m_2/(m_1+m_2)=2\mu/m_1\ . \tag{37}$$

These approximations are compared to the exact result of Eq. (34) in Fig. 2, for the typical cases of ions in an electron plasma, $m_2/m_1\cong 0$, and for equal masses, $m_2/m_1=1$.

Let us now calculate the thermal average of $G(v_1,v_2)$. Eq. (26), to find the average loss S in Eq. (25). We can approximate this integral analytically by separating the regions $0\le v_2\le v_1$ and $v_1\le v_2<\infty$, and then using the approximations of Eqs. (36a) and (36b) on each of these ranges of integration, viz.,

$$G(v_1)\cong\int_0^{v_1}G(v_1\gg v_2)N(v_2)dv_2 + \int_{v_1}^{\infty}G(v_1\ll v_2)N(v_2)dv_2\ . \tag{38}$$

For $\alpha v_1^2,\ \alpha v_2^2 \gg 1$, these two integrals give

$$G_1(v_1)=(1-\delta/2)[\phi(x)-x\phi'(x)]\ln(\alpha v_1^2)\ , \tag{39a}$$

$$G_2(v_1)=\frac{4}{3\pi^{1/2}}E_1(x^2)-\frac{\delta x}{\pi^{1/2}}[E_1(x^2)+e^{-x^2}\ln(\alpha v_1^2)] \tag{39b}$$

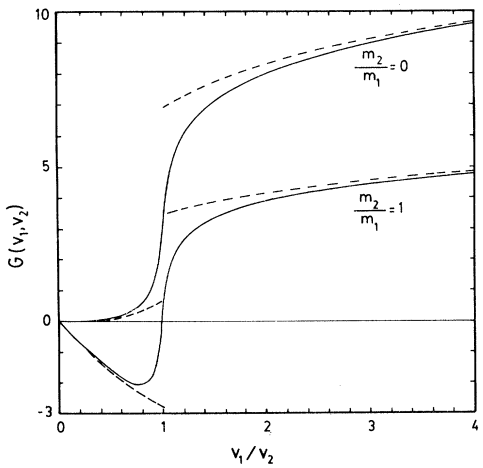

FIG. 2. Comparison between the exact and the approximate results for $G(v_1,v_2)$ for $m_2/m_1=0$ and 1, and for $\alpha=10^3$. The exact results, from Eq. (34), are shown with solid lines. The approximations for $v_1\gg v_2$, Eq. (36a), and for $v_1\ll v_2$, Eq. (36b), are shown with dashed lines.

and we finally obtain

$$G(v_1)=[(1-\delta/2)\phi(x)-x\phi'(x)]\ln(\alpha v_1^2) + \left[\frac{4x^3}{3\pi^{1/2}}-\frac{\delta x}{\pi^{1/2}}\right]E_1(x^2)\ , \tag{40}$$

in terms of the error function $\phi(x)$ and the exponential integral $E_1(y)$ defined as[28]

$$\phi(x)=\frac{2}{\pi^{1/2}}\int_0^x dt\, e^{-t^2}\ ,$$
$$E_1(y)=\int_y^{\infty}\frac{e^{-t}}{t}dt\ ,$$

and with

$$x=v_1/v_s,\quad v_s=(2k_BT/m_2)^{1/2}\ , \tag{41}$$

where s refers to a given species of plasma particles (e.g., electrons or ions).

It is of interest to show now that the result of Butler and Buckingham[6] can, in particular, be obtained from Eq. (33) with the approximation $\ln(1+\alpha^2 v_r^4)=2\ln\Lambda\cong$const. This approximation is equivalent to taking a minimum angle of scattering $\theta_{\min}\ll 1$ in such a way that $b_{\max}=2b_c/\theta_{\min}$, and $\ln\Lambda\cong\ln(2/\theta_{\min})$, where $\theta_{\min}$ is independent of v_r. This leads to

$$G(v_1,v_2)\cong\begin{cases}(1-\delta/2)\ln\Lambda\ , & v_1>v_2\\ -\dfrac{1}{2}\delta\dfrac{v_1}{v_2}\ln\Lambda\ , & v_1<v_2\end{cases} \tag{42}$$

and yields for the thermal average the well-known result[6]

$$G(v_1)\cong[(1-\delta/2)\phi(x)-x\phi'(x)]\ln\Lambda\ . \tag{43}$$

This approximation neglects an important contribution to the energy loss—the second term of Eq. (40)—due to plasma particles with velocities $v_2>v_1$. This is particularly obvious in the case of an electron plasma, $\delta\cong 0$, where Eq. (42) gives $G(v_1,v_2)\cong 0$ for $v_1<v_2$, and the thermal average yields $G(v_1)\cong F(x)\ln\Lambda$, with $F(x)=\phi(x)-x\phi'(x)$ giving the fraction of electrons with velocities smaller than v_1.

For some practical purposes, however, one could still use Eq. (43) to describe the energy loss, provided that one considers $\ln\Lambda$ as an averaged quantity whose value is calculated *a posteriori*.

In Fig. 3 we compare the analytical solution, Eq. (40), with the exact result obtained by numerical integration of Eq. (26) using the expression for $G(v_1,v_2)$ given in Eq. (34). The agreement is quite satisfactory for the case $\alpha=10^3$ shown in the figure; with increasing α values, the function $G(v_1,v_2)$ in Fig. 2 assumes a more pronounced steplike behavior at $v_1/v_2=1$ which leads to an even better agreement between the curves for $G(v_1)$ shown in Fig. 3 (the range of α values of interest goes from $\alpha\sim 10^3$ to 10^{10} for a range of plasma densities $n\sim 10^{10}$ to 10^{15} cm^{-3} and plasma temperatures $T\sim 10^3$ to 10^8 K). The curves for $m_2=m_1$ show that $G(v_1)<0$ when $x<1$; this corresponds to test particles with subthermal velocities who gain energy from the plasma. Thermal equilibrium is

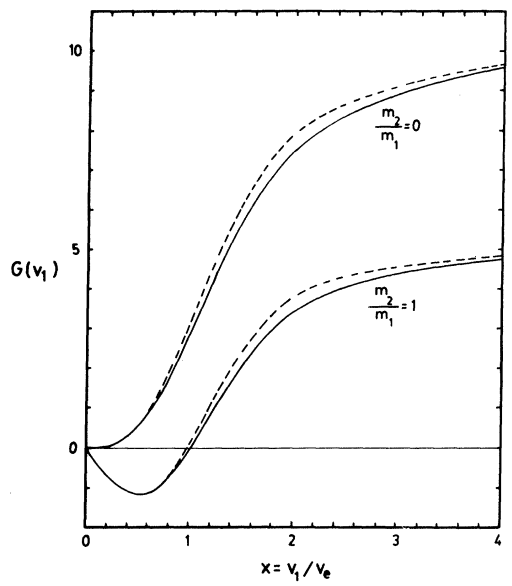

FIG. 3. Comparison of exact and approximate results for the thermal averaged function $G(v_1)$ vs the velocity ratio $x=v_1/v_s$, where $v_s=(2k_BT/m_2)^{1/2}$, for $m_2/m_1=0$ and 1, and for $\alpha=10^3$. The solid lines show the results of the numerical integration of Eq. (26) using the exact classical expression for $G(v_1,v_2)$ given by Eq. (34). The dashed lines represent the analytical approximation of Eq. (40). The negative values of the function $G(v_1)$ correspond to subthermal test particles gaining energy from the plasma until they thermalize.

reached at $x\cong 1$, when $G(v_1)=0$.

One can further simplify the result in the cases $x\ll 1$ and $x\gg 1$. For low velocities, $x\ll 1$, we can use the following limits:

$$\begin{aligned}&\phi(x)\cong 2x/\pi^{1/2}\,,\\&\phi(x)-x\phi'(x)\cong 4x^3/3\pi^{1/2}\,,\\&E_1(x)\cong\ln(1/\Gamma x)\,,\end{aligned}\tag{44}$$

with $\Gamma=e^{\gamma}\cong 1.78$ ($\gamma\cong 0.577$), which yields

$$G(v_1)\cong\frac{1}{\pi^{1/2}}\left(\tfrac{4}{3}x^3-\delta x\right)\ln\left[\frac{\alpha v_s^2}{\Gamma}\right],\quad x\ll 1\,.\tag{45}$$

The logarithmic dependence on v_1 of the first term of Eq. (40) has been cancelled out by a similar dependence of $E_1(x)$. For the case of a test ion in an electron plasma, $m_2\ll m_1$, $\delta\ll 1$, the thermalization of the ion according to Eq. (45) occurs at a value of $x\ll 1$, namely, $x^2=\frac{3}{4}\delta$, which complies with $m_1v_1^2=3k_BT$ as expected.

On the other hand, for large velocities, $x\gg 1$, we can use the limits

$$\phi(x)\cong 1,\quad \phi'(x)\to 0,\quad E_1(x^2)\to 0\tag{46}$$

and obtain

$$G(v_1)\cong(1-\delta/2)\ln(\alpha v_1^2)=(\mu/m_2)\ln(\alpha v_1^2),\quad x\gg 1\,.\tag{47}$$

The forefactor μ/m_2 leads to the right m_2 dependence of the energy loss of fast particles, namely,

$$S\cong 4\pi\frac{(Z_1Z_2e^2)^2}{m_2v_1^2}n\ln(\alpha v_1^2),\quad x\gg 1\,.\tag{48}$$

In particular, this agrees with the classical result of Bohr[22] for the energy loss of fast particles in matter, provided that we set $b_{\max}=(2/\Gamma)v_1/\omega_0$ to obtain

$$\alpha v_1^2=1.123\mu v_1^3/Z_1Z_2e^2\omega_0\,,$$

where ω_0 is the frequency of the atomic oscillators in the medium (in our case ω_0 is replaced by the plasma frequency ω_p). Using Bohr's arguments,[22] this corresponds to an adiabatic distance $\sim v_1/\omega_0$, as the range of "resonant" excitation of atoms. The high-velocity result becomes independent of the plasma temperature. The classical results of this section will be further analyzed in Sec. V.

IV. QUANTUM-MECHANICAL THEORY

In this section we describe the quantum-mechanical calculation of the transport cross section $\sigma_{\rm tr}$ for the case of an electron plasma, and we develop simple approximations which are useful to obtain analytical results for the energy loss. The results apply to the classical or quantum-mechanical domains discussed in Sec. I (hereafter $m_2=m$ is the electron mass and we set $m_2/m_1\cong 0$).

We start by considering the scattering of plasma electrons on a slow test ion, taking into account screening effects by assuming a potential of the form

$$V(r)=\frac{Z_1e^2}{r}e^{-r/\lambda_D}\,,\tag{49}$$

where λ_D is the Debye screening length. The transport cross section can be calculated in terms of the quantum phase shifts δ_l from the well-known expression

$$\sigma_{\rm tr}(k)=\frac{4\pi}{k^2}\sum_{l=1}^{\infty}l\sin^2(\delta_l-\delta_{l-1})\,,\tag{50}$$

where $k=mv_r/\hbar$ is the wave vector of the electron incident with velocity v_r relative to the scattering center.

The basis for our calculation rests on the observation that $k\lambda_D$ is very large for nearly all cases of interest.[29] Therefore, we can introduce a value L such that $1\ll L\ll k\lambda_D$. This corresponds to a distance $R=L/k$ such that $\lambda\ll R\ll\lambda_D$, where $\lambda=k^{-1}=\hbar/mv_r$, and it allows the use of different approximations for the short range, $l<L$, and distant, $l>L$, terms of the scattering problem.

(i) $l<L$. Since the value of R is taken as $R\ll\lambda_D$, the potential for all those wave components with $l<L$ can be approximated by a Coulomb potential (as in a previous calculation by De Witt[30]),

$$V(r)=\begin{cases}\dfrac{Z_1e^2}{r}, & r\le R\\ 0, & r>R\,.\end{cases}\tag{51}$$

For $r<R$ this agrees with the first term in the expansion of Eq. (49); the next term is of order $R/\lambda_D\ll 1$, and can be neglected.

The phase shifts for this potential were calculated by

Holdeman and Thaler[31] who found

$$\delta_l = \begin{cases} \arg\Gamma(l+1+i\eta)-\eta\ln(2kR)+O(\eta/kR), & l \ll L \\ 0, & l \gg L \end{cases} \quad (52)$$

where $\eta = Z_1 e^2/\hbar v_r$ is the "Bloch parameter." Here we assume that $\eta/kR \ll 1$; those cases where $\eta/kR \sim 1$, i.e.,

$$b_c = Z_1 e^2/m v_r^2 \sim R \ ,$$

will be discussed later. From this expression for δ_l we calculate

$$\delta_l - \delta_{l-1} = \arg\Gamma(l+1+i\eta)-\arg\Gamma(l+i\eta)$$
$$= \arctan(\eta/l) \ , \quad (53)$$

$$\sin^2(\delta_l-\delta_{l-1}) = \eta^2/(\eta^2+l^2) \ , \quad (54)$$

and the cross section $\sigma_{\rm tr}$, Eq. (50), becomes

$$\sigma_{\rm tr}^{(1)} = \frac{4\pi\eta^2}{k^2}\sum_{l=1}^{L}\frac{l}{l^2+\eta^2} = \frac{2\pi\eta^2}{k^2}\sum_{l=1}^{L}\left[\frac{1}{l+i\eta}+\frac{1}{l-i\eta}\right] , \quad (55)$$

where the sum can be written in terms of the digamma function $\psi(z)$ as follows[28]:

$$\sum_{l=1}^{L}\frac{1}{l+i\eta} = \sum_{q=0}^{L-1}\frac{1}{q+1+i\eta}$$
$$= \psi(L+1+i\eta)-\psi(1+i\eta) \ ,$$

and we obtain

$$\sigma_{\rm tr}^{(1)} = \frac{4\pi\eta^2}{k^2}[\ln L - {\rm Re}\psi(i\eta)] \ , \quad (56)$$

where we used the properties

$$\psi(z^*) = [\psi(z)]^* \ , \quad {\rm Re}\psi(1+i\eta) = {\rm Re}\psi(i\eta) \ ,$$

and $\psi(z) \simeq \ln z$ for $z \to \infty$.

(ii) $l > L$. The contribution from large l values can be calculated using the semiclassical approximation[32] for δ_l, which for the screened potential of Eq. (49) yields

$$\delta_l = -\frac{m}{\hbar^2}\int_{r_0}^{\infty}\frac{V(r)dr}{[k^2-(l+\frac{1}{2})^2/r^2]^{1/2}}$$
$$= -\frac{mZ_1e^2}{\hbar^2 k}\int_1^{\infty}\frac{e^{-\theta x}dx}{(x^2-1)^{1/2}} \ , \quad (57)$$

where $r_0 = (l+\frac{1}{2})/k$ and $\theta = (l+\frac{1}{2})/k\lambda_D$. The integral gives the Bessel function $K_0(\theta)$ and we get

$$\delta_l = -\frac{mZ_1e^2}{\hbar^2 k}K_0\left[\frac{l+\frac{1}{2}}{k\lambda_D}\right] . \quad (58)$$

For $l \gg 1$ we can use the property

$$dK_0(x)/dx = -K_1(x) \ ,$$

and approximate

$$\sin^2(\delta_l-\delta_{l-1}) \cong (\delta_l-\delta_{l-1})^2 \cong \left[\frac{d\delta_l}{dl}\right]^2 , \quad (59)$$

with

$$\frac{d\delta_l}{dl} \cong \frac{mZ_1e^2}{\hbar^2k^2\lambda_D}K_1\left[\frac{l+\frac{1}{2}}{k\lambda_D}\right] . \quad (60)$$

The sum of Eq. (50), for $l \gg 1$, can be transformed into an integral

$$\sigma_{\rm tr}^{(2)} = \frac{4\pi}{k^2}\left[\frac{mZ_1e^2}{\hbar^2k^2\lambda_D}\right]^2\int_L^{\infty}K_1^2\left[\frac{l+\frac{1}{2}}{k\lambda_D}\right]l\,dl \ , \quad (61)$$

and since $l+\frac{1}{2} \cong l$, the integral becomes

$$(k\lambda_D)^2\int_{L/k\lambda_D}^{\infty}xK_1^2(x)dx = \frac{L^2}{2}(K_1^2-K_0K_2)\Big|_{L/k\lambda_D}^{\infty} . \quad (62)$$

Using the limits of the Bessel functions for $x \ll 1$ (i.e., $L \ll k\lambda_D$), we obtain (with $\gamma = 0.577$)

$$\sigma_{\rm tr}^{(2)} = \frac{4\pi}{k^2}\left[\frac{mZ_1e^2}{\hbar^2k}\right]^2\left[\ln\left[\frac{2k\lambda_D}{L}\right]-\gamma-\frac{1}{2}\right] . \quad (63)$$

Finally, from Eqs. (56) and (63) we find for the transport cross section (with $k = mv_r/\hbar$):

$$\sigma_{\rm tr}(k) = \sigma_{\rm tr}^{(1)}+\sigma_{\rm tr}^{(2)}$$
$$= 4\pi\left[\frac{Z_1e^2}{mv_r^2}\right]^2$$
$$\times\left[\ln(2k\lambda_D)-{\rm Re}\psi\left[i\frac{Z_1e^2}{\hbar v_r}\right]-\gamma-\frac{1}{2}\right] , \quad (64)$$

independently of the value of L.

It is now interesting to consider the classical ($Z_1e^2/\hbar v_r \gg 1$) and quantum-mechanical ($Z_1e^2/\hbar v_r \ll 1$) limits of this expression.

A. Classical limit (CL), $Z_1e^2/\hbar v_r \gg 1$

Using the asymptotic behavior of the digamma function ${\rm Re}\psi(i\eta) \simeq \ln\eta$, $\eta \gg 1$, we obtain

$$\sigma_{\rm tr}^{\rm CL} = 4\pi\left[\frac{Z_1e^2}{mv_r^2}\right]^2\left[\ln\left[\frac{2mv_r^2\lambda_D}{Z_1e^2}\right]-\gamma-\frac{1}{2}\right] \quad (65)$$

in exact agreement with the result of a fully classical calculation.[33]

B. Quantum-mechanical (plane-wave) limit (QM or QMPW), $Z_1e^2/\hbar v_r \ll 1$

In this case we approximate $\psi(i\eta) \cong -\gamma$ for $\eta \to 0$ to obtain

$$\sigma_{\rm tr}^{\rm QM} = 4\pi\left[\frac{Z_1e^2}{mv_r^2}\right]^2[\ln(2k\lambda_D)-\tfrac{1}{2}] , \quad (66)$$

which is the result obtained using the Born approximation

in the limit $k\lambda_D \gg 1$, consistent with our case.

Thus, the result for the cross section, Eq. (64), is a general quantum-mechanical solution for the scattering of electrons in the screened potential of Eq. (49). In particular, it permits to interpolate between the classical (CL) and quantum-mechanical (QMPW) limits, much in the same way as the Bloch formula[24,25] for the energy loss of fast particles unified different results, that were previously obtained with classical[22] and quantum-mechanical[23] approximations.

However, in order for us to get the energy loss using the previous result for $\sigma_{tr}(k)$, we must still integrate over all the relative velocities $v_r = \hbar k/m$ between the moving test particle and the electrons in the plasma. Here we find two additional difficulties. The first one is that our approximation for δ_l, Eq. (52), can be applied only when $\eta/kR \ll 1$ (or $b_c \ll R \ll \lambda_D$), which is not satisfied when $k \to 0$. In addition, we want to obtain an analytical approximation for the energy loss, which is not possible using Eq. (64).

A way out of this trouble is to propose a simplified formula for the transport cross section, by introducing in the classical expression, Eq. (30), a minimum impact parameter b_{min} to take into account the quantum-mechanical corrections; this immediately yields the result

$$\sigma'_{tr} = 2\pi b_c^2 [\ln(1 + b_{max}^2/b_c^2) - \ln(1 + b_{min}^2/b_c^2)] . \quad (67)$$

The values of b_{max} and b_{min} in this formula can now be chosen so as to reproduce very closely the results of Eqs. (64)—(66). First, Eq. (64) corresponds to the limit $b_{max} \gg b_c$ of Eq. (67), namely,

$$\sigma'_{tr} \cong 2\pi b_c^2 [2\ln(b_{max}/b_c) - \ln(1 + b_{min}^2/b_c^2)]$$
$$\cong 2\pi b_c^2 [2\ln(b_{max}/b_{min}) - \ln(1 + b_c^2/b_{min}^2)] , \quad (68)$$

where $b_{max}/b_{min} \sim k\lambda_D$, and $b_c/b_{min} \sim Z_1 e^2/\hbar v_r$, as it will be shown below. Furthermore, Eqs. (65) and (66) correspond to the $b_c \gg b_{min}$ and $b_c \ll b_{min}$ limits of Eq. (68), viz.,

$$\sigma'_{tr} \cong \begin{cases} 4\pi b_c^2 \ln(b_{max}/b_c) , & b_c \gg b_{min} \quad (69a) \\ 4\pi b_c^2 \ln(b_{max}/b_{min}) , & b_c \ll b_{min} . \quad (69b) \end{cases}$$

By comparing this result with Eqs. (65) and (66) we obtain the desired values

$$b_{max} = 2e^{-(\gamma+1/2)}\lambda_D = 0.68\lambda_D ,$$
$$b_{min} = e^{-\gamma}/k = 0.56\lambda , \quad \lambda = \hbar/mv_r . \quad (70)$$

With these values, Eq. (67) can now be applied to all the previous cases.

It is interesting to notice that the same result, Eq. (67), could have also been obtained from the quantum-mechanical expression, Eq. (55), by transforming the sum into an integral in the form

$$\sigma_{tr} = \frac{4\pi\eta^2}{k^2} \sum_{l=1}^{L} \frac{l}{l^2+\eta^2} \cong \frac{4\pi\eta^2}{k^2} \int_{l_1}^{l_2} \frac{l}{l^2+\eta^2} dl \quad (71)$$

and then replacing $l_1 = kb_{min}$, $l_2 = kb_{max}$. This explains why our formula is so useful to incorporate both classical and quantum-mechanical effects.

As a further test of this approximation, we compare in Fig. 4 the results of the derived expression, Eq. (64), and of the proposed formula, Eq. (67). The agreement is remarkably good with the only exception of the region of small v_r values, where Eq. (64) gives spurious negative results (this corresponds to the range mentioned before, where $\eta/k\lambda_D \geq 1$ or $b_c \geq \lambda_D$), while the approximate formula, Eq. (67), has the proper behavior. Thus, Eq. (67) not only simplifies the forthcoming integrations, but it also describes the case where Eq. (64) fails.

Hence, our new formula for the transport cross section, Eq. (67), has the form

$$\sigma'_{tr} = \sigma_{tr}^{CL} - \Delta\sigma_{tr}^{QM} , \quad (72)$$

where σ_{tr}^{CL} is the classical result of Sec. III, Eq. (31) and the quantum-mechanical correction is given by

$$\Delta\sigma_{tr}^{QM} = -2\pi b_c^2 \ln\left[1 + \frac{b_{min}^2}{b_c^2}\right] = -2\pi b_c^2 \ln(1 + \beta v_r^2) , \quad (73)$$

with

$$\beta = (\hbar e^{-\gamma}/Z_1 e^2)^2 = (\hbar/\Gamma Z_1 e^2)^2 , \quad (74)$$

and $\Gamma = e^{\gamma} = 1.78$.

The calculation of the energy loss $S = -\langle dE/dx \rangle$, through Eqs. (22)—(26), proceeds now as in Sec. III. According to Eqs. (24) and (72) the integral over the angles of incidence will consist of two terms,

$$G(v_1, v_2) = G^{CL}(v_1, v_2) - \Delta G^{QM}(v_1, v_2) , \quad (75)$$

where $G^{CL}(v_1, v_2)$ is given by Eqs. (33) and (34) for $m_2/m_1 \cong 0$, while ΔG^{QM} becomes

$$\Delta G^{QM}(v_1, v_2) = \frac{1}{8v_1} \int_{|v_1 - v_2|}^{v_1 + v_2} dv_r \left[1 + \frac{v_1^2 - v_2^2}{v_r^2}\right] \times \ln(1 + \beta v_r^2) , \quad (76)$$

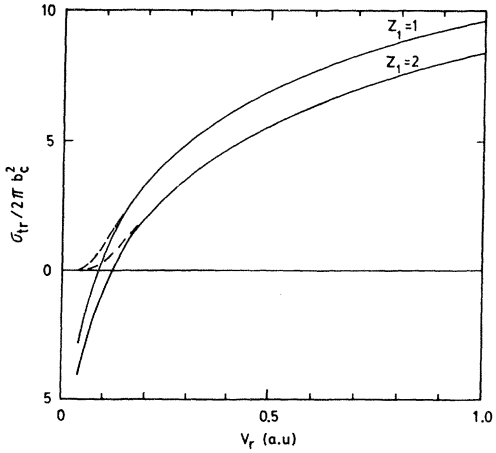

FIG. 4. Results for the transport cross section σ_{tr} vs the relative velocity v_r (in atomic units), as given by Eq. (64) (solid lines), and by Eq. (67) (dashed lines), with the values of b_{max} and b_{min} given by Eq. (70), for $\lambda_D = 200$ a.u. Equation (67) has the expected behavior for $v_r \to 0$ where Eq. (64) fails. See the text for discussion.

and by integration we obtain

$$\Delta G^{\mathrm{QM}}(v_1,v_2)=\frac{1}{8v_2}\left[2v_2[\ln(1+a^2)\pm\ln(1+b^2)]-4\begin{bmatrix}v_2\\v_1\end{bmatrix}\right.$$
$$\left.+2\beta^{1/2}\left[v_1^2-v_2^2+\frac{1}{\beta}\right][\arctan(a)-\arctan(\,|\,b\,|\,)]\right]\begin{cases}\text{for } v_1>v_2\\ \text{for } v_1<v_2\end{cases} \tag{77}$$

with $a=\beta^{1/2}(v_1+v_2)$, $b=\beta^{1/2}(v_1-v_2)$. This yields the quantum-mechanical correction to the classical results for $G(v_1,v_2)$, Eq. (34), obtained by Gryzinski.

As in Sec. III, we now calculate the limits for $v_1\gg v_2$ and $v_1\ll v_2$—but with no further approximations on the terms containing βv_1^2 and βv_2^2; this is important since we want to span the whole range of β values relative to v_1 and v_2. Thus, we obtain

$$\Delta G^{\mathrm{QM}}(v_1\gg v_2)\cong\tfrac{1}{2}\ln(1+\beta v_1^2)\,, \tag{78a}$$

$$\Delta G^{\mathrm{QM}}(v_1\ll v_2)\cong\frac{\beta v_1^3}{3v_2}\left[\frac{1}{1+\beta v_2^2}\right]. \tag{78b}$$

To integrate over the thermal distributions, we split the range of integration as in Eq. (38) and make use of the previous approximations, Eqs. (78a) and (78b), in each of those parts. Thus, we get

$$\Delta G^{\mathrm{QM}}(v_1)=\tfrac{1}{2}\ln(1+\beta v_1^2)[\phi(x)-x\phi'(x)]$$
$$+\frac{2x^3}{3\pi^{1/2}}E_1(t)\exp\left[\frac{1}{\beta v_e^2}\right], \tag{79}$$

where $t=(1+\beta v_1^2)/\beta v_e^2$, $x=v_1/v_e$, and $v_e^2=2k_BT/m$. In Fig. 5 we compare this result with the numerical integration of Eq. (26) using the exact expression, Eq. (77), and again find a very good agreement.

Our final result for an electron plasma, using Eq. (40) for the classical part (with $\delta\cong 0$, i.e., $m_2\ll m_1$) and Eq. (79) for the quantum-mechanical correction, then becomes

$$G(v_1)=\ln\left[\frac{\alpha v_1^2}{(1+\beta v_1^2)^{1/2}}\right][\phi(x)-x\phi'(x)]$$
$$+\frac{4x^3}{3\pi^{1/2}}\left[E_1(x^2)-\tfrac{1}{2}E_1(t)\exp\left[\frac{1}{\beta v_e^2}\right]\right], \tag{80}$$

where $\alpha=mb_{\max}/Z_1e^2$ and $\beta=(\hbar/\Gamma Z_1e^2)^2$.

To obtain a complete solution for the energy loss S, that can be applied to all values of $x=v_1/v_e$, we must still indicate the value of $b_{\max}$. The value in Eq. (70) was found for the case $v_1\ll v_e$, where the screening of the ion is well represented in terms of the Debye length λ_D. As discussed in Sec. I, when $v_1\sim v_e$ we can no longer use a static picture due to the appearance of dynamical many-body effects, and for $v_1\gg v_e$ the field of the ion extends over longer distances, of the order of the adiabatic length $\lambda_{\mathrm{ad}}=v_1/\omega_p$.

Since a good description of these effects cannot be given in simple terms, we will consider $b_{\max}$ as an effective velocity-dependent parameter, representing the variable range of the ion field in the plasma, in a way that reproduces all known results for low and high ion velocities. In particular, the obvious interpolation

$$b_{\max}=\frac{2}{\Gamma}\left[\frac{\lambda_D^2}{e}+\frac{v_1^2}{\omega_p^2}\right]^{1/2}=\frac{2\lambda_D}{\Gamma}\left[\frac{1}{e}+\frac{2v_1^2}{v_e^2}\right]^{1/2}, \tag{81}$$

satisfies this requirement and permits accurate calculations, as illustrated in Sec. V. It is also of interest to notice that we could obtain a similar approximation just by adding the short-range (a) and collective (b) contributions to the energy loss of a fast ion using, for instance, the results of Pines and Bohm[7]:

$$-\frac{dE^{(a)}}{dx}\cong\frac{4\pi nZ_1^2e^4}{mv_1^2}\ln\left[\frac{mv_1^2\lambda_s}{Z_1e^2}\right]$$

and

$$-\frac{dE^{(b)}}{dx}\cong\frac{2\pi nZ_1^2e^4}{mv_1^2}\ln\left[1+\frac{2v_1^2}{\langle v_2^2\rangle}\right].$$

This renders the total energy loss in approximate agreement with the use of Eq. (81) for $\lambda_s\cong 2\lambda_D/\Gamma$. We must notice, however, that Eq. (81) gives an oversimplified description of collective losses.

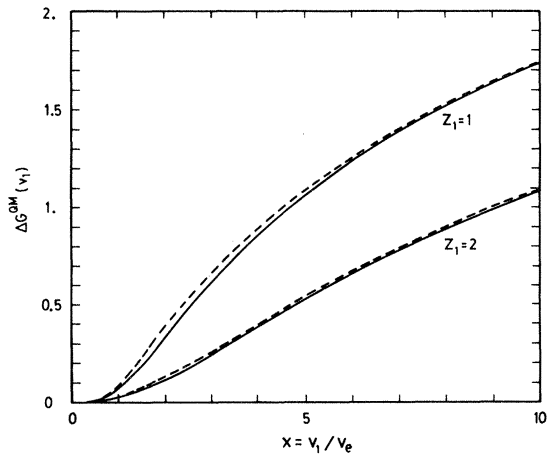

FIG. 5. Quantum-mechanical correction to the value of the function $G(v_1)$, denoted by $\Delta G^{\mathrm{QM}}(v_1)$, vs $x=v_1/v_e$, where $v_e=(2k_BT/m)^{1/2}$, for incident particles with charges $Z_1=1$ and 2, as indicated, and for $v_e=1$ ($T=13.6$ eV). The solid lines show the results of numerical integrations while the dashed lines correspond to the approximate analytical expressions of Eq. (79).

V. COMPARISON WITH PREVIOUS WORK AND DISCUSSION

A. Analysis of the results

The main result of this work is summarized by Eq. (80), which for convenience and further analysis can be cast in a form that resembles the Butler-Buckingham result[6]

$$G(v_1)=F(x)\ln\Lambda(v_1)\ , \tag{82}$$

with

$$F(x)=\phi(x)-x\phi'(x)\ , \tag{83}$$

and $x=v_1/v_e$. Thus, $F(x)$ gives the fraction of plasma electrons with velocities v_2 smaller than the particle velocity v_1. In this way, we define the velocity-dependent collision logarithm given by the expression

$$\ln\Lambda(v_1)=\ln\left[\frac{\alpha v_1^2}{(1+\beta v_1^2)^{1/2}}\right]+\frac{4x^3}{3\pi^{1/2}}\frac{[E_1(x^2)-\frac{1}{2}E_1(t)\exp(1/\beta v_e^2)]}{\phi(x)-x\phi'(x)}\ , \tag{84}$$

which condenses a wealth of information on the energy-loss problem depending on the parameters of the plasma, electron density n, and temperature T, and on the ion velocity v_1 and charge Z_1e.

By Eq. (25), the stopping power of the plasma becomes

$$S\equiv-\left\langle\frac{dE}{dx}\right\rangle=\frac{4\pi Z_1^2e^4}{mv_1^2}nF(x)\ln\Lambda(v_1)\ . \tag{85}$$

We now analyze some particular cases of interest.

1. Low velocities, $v_1 \ll v_e$

For $x=v_1/v_e\ll 1$ we can approximate

$$F(x)\cong 4x^3/3\pi^{1/2},\quad E_1(x^2)\cong\ln(1/\Gamma x^2)$$

and obtain for the stopping power

$$S\cong\frac{16\pi^{1/2}}{3}\frac{nZ_1^2e^4v_1}{m}\left[\frac{m}{2k_BT}\right]^{3/2}\ln\Lambda_1\ , \tag{86}$$

with

$$\ln\Lambda_1=\ln\left[\frac{\alpha v_e^2}{\Gamma}\right]-\frac{1}{2}E_1(t)e^t=\ln\left[\frac{4(k_BT)^{3/2}}{Z_1e^2m^{1/2}\omega_p}\right]-2\gamma-\frac{1}{2}-\frac{1}{2}E_1(t)e^t\ , \tag{87}$$

where

$$\alpha\cong\frac{2}{\Gamma e^{1/2}}\frac{m\lambda_D}{Z_1e^2},\quad t\cong\frac{1}{\beta v_e^2}\cong\left[\frac{\Gamma Z_1e^2}{\hbar v_e}\right]^2, \tag{88}$$

$\lambda_D^2=k_BT/m\omega_p^2$, and $\omega_p^2=4\pi ne^2/m$ [in Eq. (84) the limit $\beta v_1^2\to 0$ has been taken]. In Eq. (88) the factor $e^{1/2}$ corresponds to $\exp(\frac{1}{2})$ (not to be confused with the electric charge).

Equations (86) and (87) show a universal feature of low-velocity stopping powers, namely, the linear dependence on v_1; the density and temperature dependences are more complicated, although the dominant dependence is of the form $n/T^{3/2}$. The distinction between classical and quantum-mechanical (QMPW) domains appears only in the logarithmic term, through the parameter t that gives a measure of the scaled Bohr velocity, $Z_1e^2/\hbar$, relative to the thermal electron velocity $v_e=(2k_BT/m)^{1/2}$. The transition between these domains can be described by changing the temperature of the plasma. In particular, we obtain the following.

a. Low temperatures, $Z_1e^2/\hbar v_e\gg 1$. This corresponds to

$$k_BT<\tfrac{1}{2}Z_1^2me^4/\hbar^2=13.6Z_1^2$$

in eV, or $T<10^5Z_1^2$ K. Here we can take the limit $t\gg 1$ of Eq. (87), with $E_1(t)\simeq e^{-t}/t\to 0$, and obtain the classical result

$$\ln\Lambda_{\rm CL1}=\ln\left[\frac{\alpha v_e^2}{\Gamma}\right]=\ln\left[\frac{4(k_BT)^{3/2}}{Z_1e^2m^{1/2}\omega_p}\right]-2\gamma-\frac{1}{2}\ . \tag{89}$$

This agrees exactly with the result of Kihara and Aono.[13]

b. High temperatures, $Z_1e^2/\hbar v_e\ll 1$. This corresponds to $k_BT>13.6Z_1^2$ eV, or $T>10^5Z_1^2$ K. In this case $t\ll 1$ and $E_1(t)\cong-\gamma-\ln t$; then from Eq. (87) we find the quantum-mechanical result for low velocities:

$$\ln\Lambda_{\rm QM1}=\ln\left[\frac{\alpha v_e}{\beta^{1/2}}\right]-\frac{1}{2}\gamma=\ln\left[\frac{k_BT}{\hbar\omega_p}\right]+\frac{3}{2}\ln 2-\frac{1}{2}\gamma-\frac{1}{2}\ . \tag{90}$$

This is in exact agreement with the result obtained by Hamada[20] and by Arista and Brandt,[2] using the quantum-mechanical dielectric function formalism for the case of dilute plasmas [in the last reference the numerical terms of Eq. (90) have been approximated by $\frac{3}{2}\ln 2-\frac{1}{2}\gamma-\frac{1}{2}\cong\frac{1}{4}$].

2. High velocities, $v_1 \gg v_e$

For $x=v_1/v_e\gg 1$ we approximate $F(x)\cong 1$, and find

$$S\equiv-\left\langle\frac{dE}{dx}\right\rangle\cong\frac{4\pi nZ_1^2e^4}{mv_1^2}\ln\Lambda_2\ , \tag{91}$$

where

$$\ln\Lambda_2=\ln[\alpha v_1^2/(1+\beta v_1^2)^{1/2}]=\ln\left[\frac{2}{\Gamma}\frac{mv_1^3}{Z_1e^2\omega_p}\right]-\frac{1}{2}\ln\left[1+\left[\frac{\hbar v_1}{\Gamma Z_1e^2}\right]^2\right]=\ln\left[\frac{2mv_1^2}{\hbar\omega_p}\right]-\frac{1}{2}\ln\left[1+\left[\frac{\Gamma Z_1e^2}{\hbar v_1}\right]^2\right]\ , \tag{92}$$

with

$$\alpha\cong\frac{2}{\Gamma}\frac{mv_1}{Z_1e^2\omega_p},\quad \beta=(\hbar/\Gamma Z_1e^2)^2\ . \tag{93}$$

It is interesting to compare the last expression of $\ln\Lambda_2$ with the Bloch formula[24,25,34]

$$L_{\text{Bloch}}=\ln\left[\frac{2mv_1^2}{I}\right]-\gamma-\text{Re}\psi\left[i\frac{Z_1e^2}{\hbar v_1}\right]. \tag{94}$$

This provides an accurate analytical approximation for $\text{Re}\psi(i\eta)$ as shown in the Appendix.

Hence, Eq. (92) can be used to describe the transition between classical and quantum-mechanical results for fast ions in a plasma. In particular, we obtain two well-known results in the following cases.

a. Case $Z_1e^2/\hbar v_1 \gg 1$. From Eq. (92) we obtain the classical result for fast ions[22,25]:

$$\ln\Lambda_{\text{CL2}}=\ln(\alpha v_1^2)=\ln\left[\frac{2}{\Gamma}\frac{mv_1^3}{Z_1e^2\omega_p}\right]. \tag{95}$$

b. Case $Z_1e^2/\hbar v_1 \ll 1$. This leads to the quantum-mechanical expression

$$\ln\Lambda_{\text{QM2}}=\ln\left[\frac{\alpha v_1}{\beta^{1/2}}\right]=\ln\left[\frac{2mv_1^2}{\hbar\omega_p}\right], \tag{96}$$

which is the result obtained by Lindhard[9] for fast ions in a degenerate electron plasma (the degeneracy of the plasma plays no role for high ion velocities). This also corresponds to the result of Bethe[23] for the stopping power of atoms, by replacing the mean excitation potential of the Bethe theory I, with the plasmon energy $\hbar\omega_p$.

In Figs. 6(a) and 6(b) we illustrate these various approximations. They show the transition from the classical (CL1, CL2) to the quantum-mechanical (QM1, QM2) approximations, with increasing *relative* velocities between the ion and the electrons in the plasma. At low velocities $v_1 \ll v_e$ Fig. 6(a), this is illustrated by plotting $\ln\Lambda_1$, given by Eq. (87), *versus* the plasma temperature $T \propto v_e^2$. For high velocities $v_1 \gg v_e$ similar results are obtained in terms of $\ln\Lambda_2$, Eq. (92), with increasing v_1 as shown in Fig. 6(b).

We can obtain further useful expressions from Eq. (84) by taking the limits in a different order. Thus, we can consider the limits $\beta\to 0$ and $\beta\to\infty$, which yield, respectively, the classical and quantum-mechanical (QMPW) results, namely,

$$\ln\Lambda_{\text{CL}}=\ln(\alpha v_1^2)+\frac{4x^3}{3\pi^{1/2}}\frac{E_1(x^2)}{F(x)}, \tag{97}$$

$$\ln\Lambda_{\text{QM}}=\ln\left[\frac{\alpha v_1}{\beta^{1/2}}\right]+\frac{2x^3}{3\pi^{1/2}}\frac{E_1(x^2)}{F(x)}. \tag{98}$$

These expressions apply now through the whole range of x values. In particular, we retrieve the previous results, namely, $\Lambda_{\text{CL}}\cong\Lambda_{\text{CL1}}$, $\Lambda_{\text{QM}}\cong\Lambda_{\text{QM1}}$ for $x\ll 1$, and $\Lambda_{\text{CL}}\cong\Lambda_{\text{CL2}}$, $\Lambda_{\text{QM}}\cong\Lambda_{\text{QM2}}$ for $x\gg 1$, as given in Eqs. (89), (90), (95), and (96). Hence, Eqs. (97) and (98) describe the transition between low-velocity and high-velocity collision logarithms. This is illustrated in Fig. 7, where we show $\ln\Lambda_{\text{CL}}$ and $\ln\Lambda_{\text{QM}}$ as a function of $x=v_1/v_e$. For $x\ll 1$ we obtain the low-velocity results, independent of v_1, while for $x\gg 1$ the v_1 dependence becomes of the form $\ln(av_1^3)$ and $\ln(bv_1^2)$, respectively.

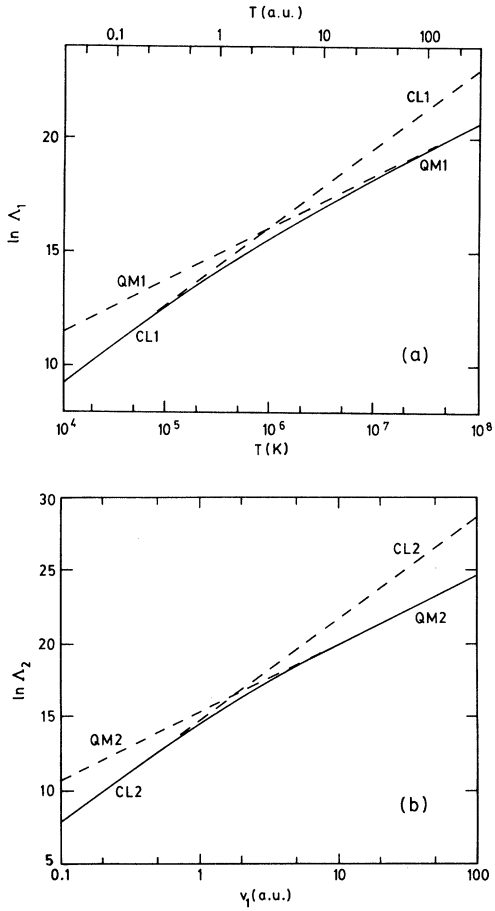

FIG. 6. The transition between the classical limit (CL) and the quantum-mechanical (plane-wave) limit (QM), as it occurs with increasing *relative* velocity between the test particle (with $Z_1=1$) and the electrons in the plasma (with density $n=10^{11}$ cm^{-3}). This is illustrated in (a) for low velocities $v_1\ll v_e$ where the transition is obtained by increasing the temperature of the plasma. (b) shows the analogous case of high velocities, $v_1\gg v_e$, and where the velocity of the test particle is increased. The solid lines are the results for $\ln\Lambda_1$ and $\ln\Lambda_2$ obtained from Eqs. (87) and (92). The lines of dashes for Λ_{CL1}, Λ_{QM1}, Λ_{CL2}, and Λ_{QM2} correspond to Eqs. (89), (90), (95), and (96).

B. Comparison with previous results

As shown before, all known analytical expressions can be retrieved as limiting cases of Eq. (84). That is already a check of the agreement with previous work. We can extend this study by comparing our results with the analysis given in a series of papers by Hamada *et al.*[19–21] They have given a complete solution to the energy-loss calculation which was expressed in terms of auxiliary tabulated functions. This provides a useful framework to ascertain the accuracy of the analytical approximations given in this paper.

First we consider the result for $\ln\Lambda_1$, Eq. (87), for $v_1\ll v_e$ and define

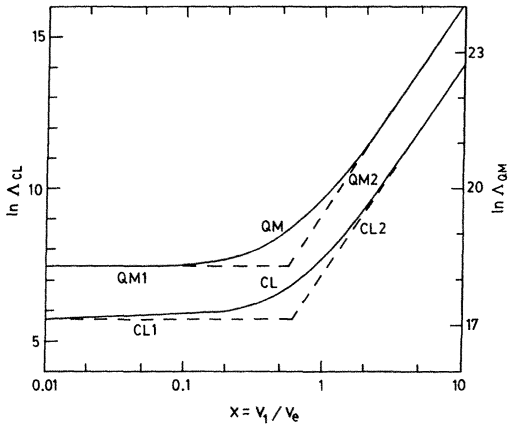

FIG. 7. Classical (left scale) and quantum-mechanical (right scale) expressions for $\ln\Lambda_{CL}$ and $\ln\Lambda_{QM}$, vs reduced velocity $x=v_1/v_e$. The solid lines correspond to the expressions of Eqs. (97) and (98). The low- and high-velocity limits, CL1,QM1 and CL2,QM2, are shown with dashed lines. Calculations correspond to electron density $n=10^{11}$ cm^{-3} and plasma temperatures $T=10^3$ K (for the classical case) and $T=10^7$ K (quantum-mechanical case).

$$\Delta L_1=\ln\Lambda_1-\ln\Lambda_{QM1}\ , \tag{99}$$

where $\ln\Lambda_{QM1}$ is the quantum-mechanical limit given by Eq. (90). This gives for ΔL_1

$$\Delta L_1=-\tfrac{1}{2}E_1(t)e^t-\tfrac{1}{2}\gamma-\tfrac{1}{2}\ln t\ , \tag{100}$$

where now

$$t=\frac{1}{\beta v_e^2}=\frac{m}{2k_BT}\left[\frac{\Gamma Z_1e^2}{\hbar}\right]^2 . \tag{101}$$

The function $-\Delta L_1$ is shown in Fig. 8(a) (solid line) as a function of the parameter $\eta=Z_1e^2/\hbar v_e$—i.e., $t=(\Gamma\eta)^2$. This corresponds to the transition between the quantum-mechanical (QM1) and the classical (CL1) expressions for $\eta\ll1$ and $\eta\gg1$, respectively. It is compared with the result of George, Okamoto, Nakamura, and Hamada,[21] $-\Delta L_1^{GONH}=\gamma+\Lambda^{GONH}(\eta)$ (dashed line) in terms of the tabulated function $\Lambda^{GONH}(\eta)$ (from Table 2 of Ref. 21; our parameter η corresponds to the parameter ν of this reference). The figure illustrates the accuracy of the analytical approximation.

A similar analysis is made for $\ln\Lambda_2$, Eq. (92) for $v_1\gg v_e$ in terms of

$$\Delta L_2=\ln\Lambda_2-\ln\Lambda_{QM2}\ , \tag{102}$$

with Λ_{QM2} given by the Bethe-Lindhard formula, Eq. (96). This gives

$$\Delta L_2=-\ln(1+t_1)^{1/2} \tag{103}$$

with

$$t_1=\frac{1}{\beta v_1^2}=\left[\frac{\Gamma Z_1e^2}{\hbar v_1}\right]^2 . \tag{104}$$

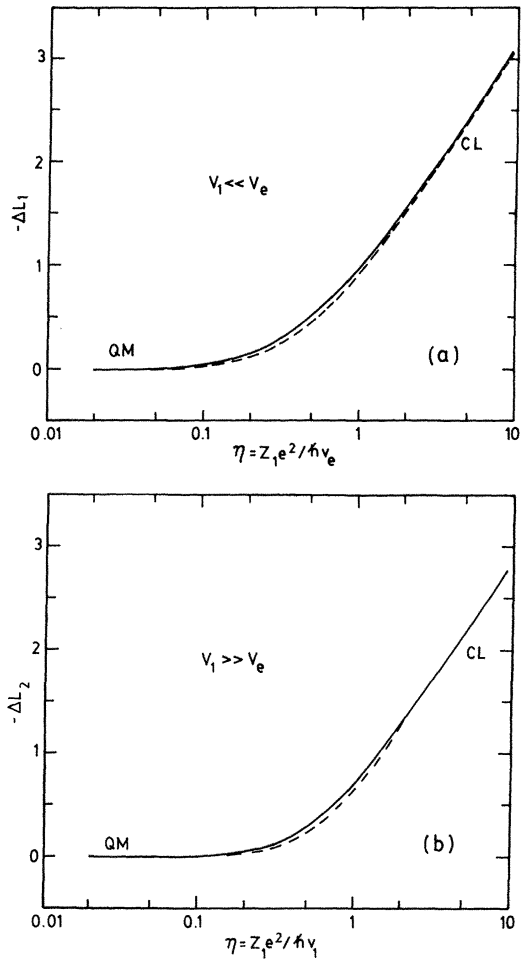

FIG. 8. Comparison between analytical and numerical results for the corrections to the quantum-mechanical collision logarithm (plane-wave approximation) due to classical effects arising for large values of η. Our results, from Eqs. (100) and (103), are shown with solid lines. In case (a), for $v_1\ll v_e$, $\eta=Z_1e^2/\hbar v_e=Z_1e^2m^{1/2}/\hbar(2k_BT)^{1/2}$; the line of dashes gives the results tabulated in Ref. 21. In case (b), for $v_1\gg v_e$, $\eta=Z_1e^2/\hbar v_1$, the dashed line corresponds to Ref. 19.

In Fig. 8(b) we compare $-\Delta L_2$ with the result of George and Hamada[19] (which is also in agreement with Bloch), namely,

$$-\Delta L_2^{GH}=\gamma+\mathrm{Re}\psi(i\eta)\ ,$$

as a function of the parameter $\eta=Z_1e^2/\hbar v_1$—hence, $t_1=(\Gamma\eta)^2$. The agreement is again excellent, as we could expect owing to the approximation

$$\mathrm{Re}\psi(ix)\cong\ln(1+\Gamma^2x^2)^{1/2}-\gamma\ ,$$

obtained in the Appendix.

To complete the comparison we consider now the results for $\ln\Lambda_{CL}$ and $\ln\Lambda_{QM}$. We define

$$\Delta L_{CL}=\ln\Lambda_{CL}(v_1)-\ln\Lambda_{CL1}\ , \tag{105}$$

$$\Delta L_{QM}=\ln\Lambda_{QM}(v_1)-\ln\Lambda_{QM1}\ , \tag{106}$$

where Λ_{CL1} and Λ_{QM1} are given by Eqs. (89) and (90). In Fig. 9 we show the results for ΔL_{CL} and ΔL_{QM} obtained using our approximations, Eqs. (97) and (98) (solid lines), and using the expressions of Hamada,[20] namely,

$$\ln\Lambda_{CL}^{H}=\ln\left[\frac{4(k_BT)^{3/2}}{Z_1e^2\omega_p m^{1/2}}\right]+\Delta_1(x)+\Delta_2(x)+1.116\ , \tag{107}$$

$$\ln\Lambda_{QM}^{H}=\ln\left[\frac{4k_BT}{\hbar\omega_p}\right]+\Delta_1(x)+\tfrac{1}{2}\Delta_2(x)+\tfrac{1}{2}\ , \tag{108}$$

where $\Delta_1(x)$ and $\Delta_2(x)$ are the functions tabulated by May[17]; these results are shown in dashed lines. The agreement is here less satisfactory at intermediate velocities, $x\sim 1$, where our approximations overestimate the value of $\ln\Lambda$. Since in most cases of interest $\ln\Lambda \gg 1$, the accuracy obtained for intermediate velocities, of order $(\ln\Lambda)^{-1}$, will still be good.

We finally notice that using in Eqs. (107) and (108) the limits of the functions calculated by May, for $x\to 0$ $[\Delta_1\cong -\frac{1}{2},\ \Delta_2\cong -(1+\gamma+\ln 2)]$ and for $x\to\infty$ $(\Delta_1\cong \ln x+\frac{1}{2}\ln 2,\ \Delta_2\cong 2\ln x-1-\ln 2)$, we find an exact agreement with the results obtained here—Eqs. (89), (90), (95), and (96).

C. Comparison with experimental results

In a series of experiments Brown *et al.*[35] have been able to obtain results for the energy loss in an ionized plasma, which for the first time cover the whole range of x values of interest, throughout the maximum of the dE/dx curve. In Fig. 10 we show the results for hydrogen ions in a singly ionized cesium plasma at temperature $T=2100$ K and electron density $n=10^{11}$ electrons/cm^3. This is a good example of the classical case, Eq. (97), both because of the ion velocity, $v_1 \ll Z_1e^2/\hbar$, and the plasma temperature, $T\ll 10^5$ K. Moreover, in these conditions, the residual contribution to the stopping power due to the core of the Cs^+ ions can be estimated to be negligible. Hence, these experiments serve as a good check of our results in the classical limit, and for the relevant range of x values.

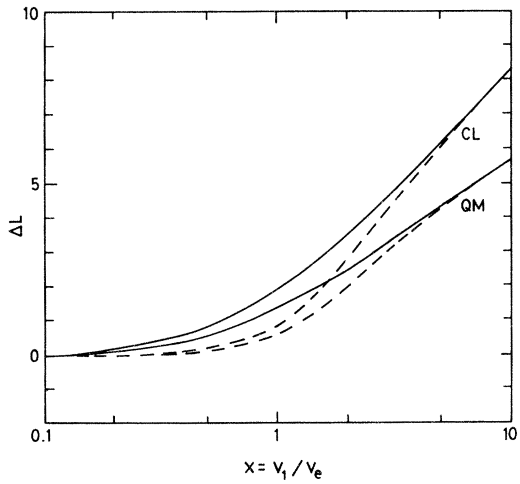

FIG. 9. Velocity-dependent part of the collision logarithm in the classical and quantum-mechanical approximations from Eqs. (105) and (106), vs $x=v_1/v_e$, with $v_e=(2k_BT/m)^{1/2}$. The dashed lines give the numerical results of Ref. 20.

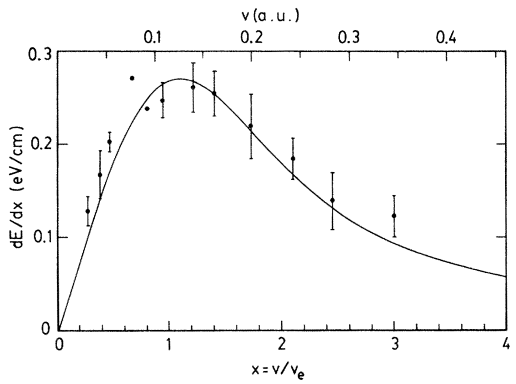

FIG. 10. Experimental results of Ref. 35 for the energy loss of hydrogen ions in a cesium plasma of density $n=10^{11}$ cm^{-3} and temperature $T=2100$ K. The solid line gives the result of this paper, Eqs. (84) and (85).

It would be important to extend this comparison to the quantum-mechanical case, particularly for light ions in hot fusion plasmas, where no similar data have so far been produced.

VI. SUMMARY AND CONCLUSIONS

We have calculated the rate of energy loss of ions in dilute plasmas using classical and quantum-mechanical treatments. The analysis is carried over by introducing several analytical approximations, based on physical grounds, and preserving at each step the accuracy of the calculation.

This procedure leads to a final analytical result, Eqs. (84) and (85), which embodies all the cases of interest for the energy loss of heavy ions in nondegenerate electron plasmas. This includes the cases of low and high velocities ($v_1 \ll v_e$, $v_1 \gg v_e$) as well as the classical and quantum-mechanical limits ($Z_1e^2/\hbar v_r \gg 1$, $Z_1e^2/\hbar v_r \ll 1$, where v_r represents a relative velocity).

The forefactor $F(x)$ in Eq. (85) contains the more obvious velocity and temperature dependences; it leads to $S\propto nZ_1^2v_1/T^{3/2}$ at low velocities, Eq. (86), and to $S\propto nZ_1^2/v_1^2$ at high velocities, Eq. (91). This explains also the maximum of the energy-loss function in simple terms. On the other hand, the velocity dependent collision logarithm, as defined in Eq. (84), incorporates quantum-mechanical corrections and the residual velocity dependence that arises from close and distant collisions. Hence, it is a more complex function of v_1, Z_1, n and T.

In Fig. 11 we give a summary of the various cases comprised in our description. Here CL1 and CL2 represent conditions of applicability of the classical approximations of Eqs. (89) and (95), whereas QM1 and QM2 indicate the cases where the quantum-mechanical approximations of Eqs. (90) and (96) apply. The arrows represent the directions of increasing ion velocity v_1 or increasing plasma temperature T. Also indicated on each

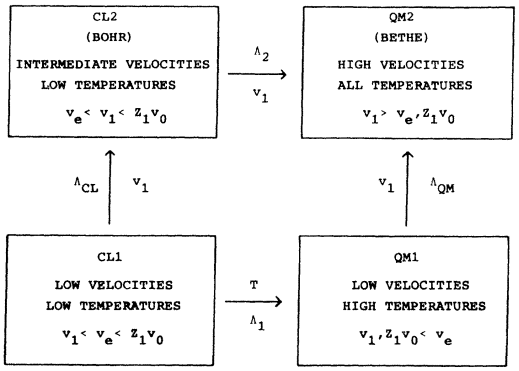

FIG. 11. Summary of the cases included in our analysis of the energy loss of ions in an electron plasma. CL1, CL2, QM1, and QM2 correspond to the limiting cases of Eqs. (89), (95), (90), and (96). The directions of increasing ion velocity v_1 or plasma temperature T are indicated. The transitions between these various limits are described by Λ_1, Λ_2, Λ_{CL}, and Λ_{QM}, according to Eqs. (87), (92), (97), and (98). All these approximations are contained in the analytical result for the collision logarithm, Eq. (84), as a function of the ion charge $Z_1 e$ and velocity v_1, and of the plasma density n and temperature $T = \frac{1}{2} m v_e^2 / k_B$. Here $v_0 = e^2/\hbar$ is Bohr velocity.

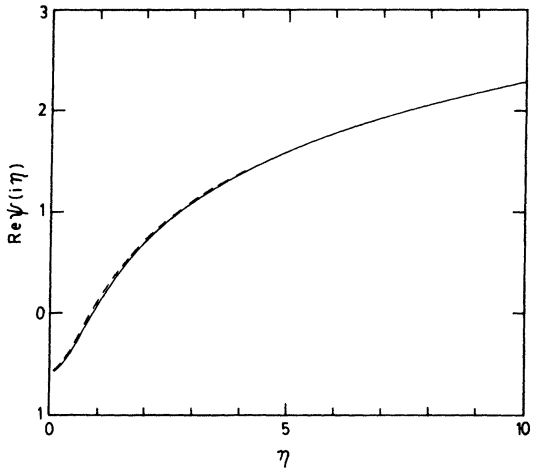

FIG. 12. Results for the real part of the digamma function of imaginary argument $\psi(i\eta)$ as obtained from Eq. (A1) (dashed line) and exact values obtained from tables (Ref. 28) (solid line).

side is the approximation for the collision logarithm that describes the transition between the corresponding cases. Thus, for instance, by increasing the temperature, with a fixed ion velocity $v_1 \ll v_e$, we go from the classical low-temperature case, CL1, to the quantum-mechanical high-temperature limit, QM1. This transition is described by the approximation denoted as $\ln\Lambda_1$ and given in Eq. (87). In a similar way, the expression for Λ_2, Λ_{CL}, and Λ_{QM}, Eqs. (92), (97), and (98), connect the other limiting cases. These are all approximations of the general result of Eq. (84).

The agreement with experimental results is satisfactory, but it only covers a limited domain of the analysis given here. One of the basic problems described in this paper is the transition between classical and quantum-mechanical approximations. This is particularly important to describe the effects due to the penetration of light and heavy ion beams in fusion plasmas. In this sense it would be of much interest to test the theoretical predictions with energy-loss experiments in ionized plasmas, under the extreme conditions of high temperatures required for thermonuclear research.

ACKNOWLEDGMENTS

One of us (L. de F.) is grateful to the Consejo Nacional de Investigaciones Científicas y Técnicas, for a research fellowship.

APPENDIX

The comparison of our result for $v_1 \gg v_e$, Eq. (92), with the corresponding limit given by the Bloch formula of Eq. (94) provides an approximating expression for $\mathrm{Re}\psi(i\eta)$, namely,

$$\mathrm{Re}\psi(i\eta) \cong -\gamma + \tfrac{1}{2}\ln(1+\Gamma^2\eta^2) , \qquad \text{(A1)}$$

with $\Gamma = \exp\gamma = 1.781$.

In Fig. 12 we compare this approximation (dashed line) with the exact values of $\mathrm{Re}\psi(i\eta)$ (solid line). Owing to the wide range of applicability of the Bloch solution we consider this result of considerable practical value.

[1]Proceedings of the Informal Workshop on the Penetration of Charged Particles in Matter Under Extreme Conditions, New York University, January 1980 (unpublished).
[2]N. Arista and W. Brandt, Phys. Rev. A 23, 1898 (1981).
[3]L. Spitzer, Jr., *Physics of Fully Ionized Gases* (Interscience, New York, 1962).
[4]S. Chandrasekhar, Astrophys. J 93, 285 (1941).
[5]M. Gryzinski, Phys. Rev. 107, 1471 (1957).
[6]S. T. Butler and M. J. Buckingham, Phys. Rev. 126, 1 (1962).
[7]D. Pines and D. Bohm, Phys. Rev. 85, 338 (1952).
[8]A. I. Akhiezer and A. G. Sitenko, Zh. Eksp. Teor. Fiz. 23, 161 (1952); A. G. Sitenko, *Electromagnetic Fluctuations in Plasma* (Academic, New York, 1967); A. I. Akhiezer, I. A. Akhiezer, R. V. Polovin, A. G. Sitenko, and K. N. Stepanov, *Plasma Electrodynamics* (Pergamon, New York, 1975), Vol. 2.
[9]J. Lindhard, K. Dan. Vidensk. Selsk. Mat. Fys. Medd. 28, No. 8 (1954).
[10]R. H. Ritchie, Phys. Rev. 114, 644 (1959).
[11]S. Skupsky, Phys. Rev. A 16, 727 (1977).
[12]G. Maynard and C. Deutsch, Phys. Rev. A 26, 665 (1982).
[13]T. Kihara and O. Aono, J. Phys. Soc. Jpn. 18, 837 (1963).
[14]T. Kihara, O. Aono, and Y. Itikawa, J. Phys. Soc. Jpn. 18, 1043 (1963).
[15]T. Kihara, J. Phys. Soc. Jpn. 19, 108 (1964).
[16]Y. Itikawa and O. Aono, Phys. Fluids 9, 1259 (1966).
[17]R. M. May, Aust. J. Phys. 22, 687 (1969).

[18]J. Hubbard, Proc. Roy. Soc. London Ser. A 261, 371 (1961).
[19]E. P. George and T. Hamada, Phys. Lett. 67A, 369 (1978).
[20]T. Hamada, Aust. J. Phys. 31, 291 (1978).
[21]E. P. George, K. Okamoto, Y. Nakamura, and T. Hamada, Aust. J. Phys. 32, 223 (1979).
[22]N. Bohr, Philos. Mag. 25, 10 (1913).
[23]H. Bethe, Ann. Phys. (Leipzig) 5, 325 (1930).
[24]F. Bloch, Ann. Phys. (Leipzig) 16, 285 (1933).
[25]S. P. Ahlen, Rev. Mod. Phys. 52, 121 (1980).
[26]A. Bohr, K. Dan.Vidensk. Selsk. Mat. Fys. Medd. 24, No. 19 (1948).
[27]J. Neufeld and R. H. Ritchie, Phys. Rev. 98, 1632 (1955).
[28]*Handbook of Mathematical Functions,* edited by M. Abramowitz and I. A. Stegun (Dover, New York, 1970); I. S. Gradshtein and I. M. Ryzhik, *Table of Integrals, Series and Products* (Academic, New York, 1965).
[29]For slow ions $v_r \sim v_e$, and since $\lambda_D \simeq v_e/\omega_p$ we get $k\lambda_D \simeq mv_e^2/\hbar\omega_p \sim k_B T/\hbar\omega_p \gg 1$. Thus, $k\lambda_D \gg 1$ for most of the electrons in the distribution.
[30]H. De Witt, in *Lectures in Theoretical Physics,* edited by W. E. Brittin (Gordon and Breach, New York, 1967), Vol. IX-C.
[31]J. T. Holdeman and R. M. Thaler, Phys. Rev. 139B, 1186 (1965).
[32]L. D. Landau and E. M. Lifshitz, *Quantum Mechanics: Non-Relativistic Theory* (Pergamon, New York, 1977).
[33]R. L. Liboff, Phys. Fluids 2, 40 (1959).
[34]R. J. Gould, Phys. Lett. 36A, 485 (1971).
[35]D. M. Cox, H. H. Brown, Jr., I. Klavan, and B. Bederson, Phys. Rev. A 10, 1409 (1974); D. Taggart, L. Schumann, and H. H. Brown, Jr., Phys. Fluids 24, 1180 (1981).